Assessing Statistical Downscaling to quantify the Impact of Climate Changes of Rainfall over the Blue Nile Basin

HanyMostafa¹, Hazem Saleh², Mahmoud El Sheikh² and Khaled Kheireldin¹

¹Department of Environmental Studies, Environment and Climate changes Research Institute, National Water Research Center Building El-Qanater El-Khairiya, Egypt, ²Civil Engineering Department, Faculty of Engineering, Minoufiya University, Egypt, E. meil: henv. maustafo@hatmail.com

E-mail: <u>hany_moustafa@hotmail.com</u>

Abstract: Statistical downscaling methods were used to investigate the impact of climate change on rainfall of the Blue Nile Basin to assess the projected precipitation changes for the intermediate and end of 21st century in a way that is relevant to water-resource decision making. The applied downscaling methods are scaling approach correction and quantile mapping approach correction. These were applied on 16 GCM runs with A2 emission scenario. The future simulations were conducted for 2020s (2011-2039), 2050s (2041-2070) and 2080s (2071-2100) horizons representing near, intermediate and far future, respectively and were compared with 1970–2000 CRU nominal period. The outcomes of these sixteen GCMs were ranked to provide average future changes. The downscaling involved linear multiple regression analysis and was carried out using a number of downscaling and climate data manipulation tools, Xlstat. Regression analysis have been used to test the performance of the models. The accuracy and performance of downscaled values of rainfall has been quantified in terms of the root mean square error (RMSE) and coefficient of determination (R^2). The minimum and maximum monthly rainfall change for the Blue Nile were -1,89% and +63.57%, -5.96% and +69.37%, and -8.9% and +76.44% for future periods 2010–2039, 2040-2069 and 2070-2099, respectively. However, the Met Office Hadley Centre, UK (HADGEM) was found to be the best performance model to simulate the projected rainfall over the Blue Nile followed by CGMR, BCM2, MRCGM and CNCM3. The mean monthly rainfall of HADGEM downscaling were -1.87%, +1.62% and +4.71% of observed historical rainfall (1971-2000) for future periods of 2020s (2010-2039), 2050s (2040-2069) and 2080s (2070–2099). The correlation coefficient, R2 and RMSE for the mean monthly precipitation (MAP) for the best performance model HADGEM were 0.98%, 0.96% and 18.23 mm/month. This study provides useful information to decision makers for the planning and management of future water resources of the study area and downstream countries.

[Hany Mostafa, Hazem Saleh, Mahmoud El Sheikh and Khaled Kheireldin. Assessing Statistical Downscaling to quantify the Impact of Climate Changes of Rainfall over the Blue Nile Basin. *Life Sci J* 2015;12(12):86-95]. (ISSN:1097-8135). <u>http://www.lifesciencesite.com</u>. 12. doi:<u>10.7537/marslsj121215.12</u>.

Keyword: Statistical downscaling, climate changes, precipitation, rainfall, Global Circulation Models (GCMs)

1. Introduction

Climate change is nowadays recognized as a global challenge and issue of our times. [United Nations Secretariat, 2007], climate change impacts could be severe for society. However, the Intergovernmental Panel on Climate Change (IPCC) Fifth Assessment Report concludes that climate change is real and its impacts is already being felt and action needs to be taken [IPCC, 2014]. Warming temperatures are projected to cause frequent and extreme weather events, such as heavy rainstorms, flooding, and El Nino events [IPCC, 2001]. The Third Assessment Report (TAR) observed that temperatures have shown an increased warming trend since the 1960s. Rainfall in the Eastern Nile Basin exhibits significant spatial and temporal variability [Hulme et al., 2005]. Rainfall and river flow records during the 20th century reveal high levels of inter-annual and inter-decadal variability. Moreover, significant fluctuations in rainfall have occurred in the humid

headwaters of the Ethiopian highlands over decadal timescales with marked consequences for Nile flows *[Conway, 2005]*. The topographic characteristics of some parts of the Eastern Nile Basin make them vulnerable to flooding. During exceptionally wet years, high discharge from the Blue Nile, Atbara and the Sobat result in large scale flooding in the floodplain areas of southeastern Sudan. The impacts of flooding include loss of human life, crops, livestock, increased risk of disease transmission (Rift Valley Fever, malaria, cholera) and damage to physical infrastructure, especially roads.

Global Climate Models (GCMs) are the primary tools for simulating the present climate and understanding how the global climate may change in the future *[Kundzewicz et.al. 2007]*. The atmospheric or oceanic GCMs (Atmospheric General Circulation Model AGCM or Ocean General Circulation Model OGCM) are key components of GCMs which include land-surface, sea-ice and ocean components. Twentyfour GCMs are available to simulate climate change scenarios in the future. In many studies rainfall downscaled from some GCMs for current climate is compared with the observed historical rainfall to access model reliability [Whitehead et al., 2006; Perkins et al., 2007; Chiew et al., 2009, Chiew et al., 2010; Timbal et al., 2009. Data generation by downscaling GCM output will be one of the options to know the future rainfall condition in the particular region. However, their resolution in longitude and latitude is generally too low (not less than about 300 km spatial scale, [Mearns et al., 2001 and Christensen et al., 2007] to be adapted to local impacts. Then, GCMs become unable to depict details needed for assessing climate change impacts at national and regional level. Therefore, climate scientists simulate regional changes by zooming in on global models using the same equations, but solving them for a much larger number of grid points in particular locations [Schiermeier, 2010].

Basically, two fundamental techniques were developed for downscaling of coarse GCM simulations to finer resolutions; dynamical and statistical downscaling. Statistical downscaling techniques, which relate large-scale climate variables. are grouped under three classes; regression methods, weather typing (classification) and weather generators. It can serve as a tool to generate synthetic weather data required for climate change impact assessment studies [Wilby et al., 2002; Harpham & Wilby, 2005; Khan et al., 2006]. In regression-based downscaling methods either linear or nonlinear relationships between the predictors and the predictand of interest are developed. Bias correction method of downscaling minimizes the biases of GCM outputs for each of the grids. The bias correction methods largely eliminate the error of the GCM with added emphasis on statistical characteristics of observation data. The Intergovernmental Panel on Climate Change (IPCC) 4th Assessment Report (AR4) found that 18 of 21 Global Climate Models (GCMs) agree on increased precipitation in eastern Africa [Christensen, et al., 2007]. Earlier analysis making use of 17 different GCMs revealed an average increase in temperature over the basin by 2 to 5 C° by 2090 [Elshamy, et al., 2009].

The aim of this study was to assess the impact of climate change on rainfall over the Blue Nile by predicting future ensemble rainfall using 16 GCMS with A2 scenario with the help statistical downscaling tool. Furthermore, the manuscript/paper presents an analysis of monthly, seasonal and annual changes in rainfall pattern in the Eastern River Basin.

2. Study Area and Input Data

The Blue Nile sub basin is one of the four major sub-basins in the Eastern Nile Basin. It is located

between 16^{0} 2' N and 7⁰ 40' N latitude, and 32^{0} 49' E and 39^{0} 30' E longitude and has a total area of 311,548 square kilometers (65% in Ethiopia and 35% in Sudan) *[Peggy and* Curtis, *1994]*, as shown in Figure 1. The Blue Nile Basin comprises only 8% of the total Nile Basin catchment area, on average; the Blue Nile contributes almost 60% of the Main Nile River flow at Aswan Dam in Egypt. *[Gebrehiwot et al., 2011]*.

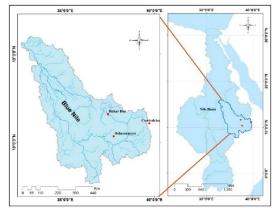


Figure 1. Location Map of the Study Area- Blue Nile Basin

Approximately 7% of the water flow of the Blue Nile comes from Lake Tana itself [Whittington, 1983], while 70% of the runoff occurs between July and September. Peaking in August, after which the Blue Nile start to fall as rain water supply to the river begins to decline [Mishra et. al, 2003]. The Blue Nile basin can be characterized as a hilly area. The Blue Nile River emanates from Lake Tana in Ethiopia at an elevation of 1780 ma.s.l. Approximately 30 km downstream of Lake Tana, at the Blue Nile falls the river drops into a deep gorge and travels about 940 km till the Ethiopian-Sudanese boarder [Conway, 1997]. The Blue Nile and the White Nile join each other in Khartoum to form the Main Nile River that flows northeast. After 322 km the Nile River is joined by the Atbara River and continues its course up to Egypt where it enters Lake Nasser and flows further downstream to enter the Nile Delta before reaching the Mediterranean Sea.

The climate of the study area varies from humid to semiarid. The basin comprises two different climatic zones: the humid Ethiopian highlands, characterized by high rainfall and low temperatures in the wet season (July-August-September), and the semi-arid South-East Sudan, with low rainfall and high temperatures throughout the entire year [Shahin, 1985]. Most precipitation occurs in the wet season (June through September), and the remaining precipitation occurs in the dry season (October through January or February) and in the mild season (February or March through May). The mean annual rainfall varies from 2,200 mm in the Didessa and Dabus sub-basins to 900 mm near the Ethiopian Sudanese border and decreases to less than 200 mm in Khartoum. However, the mean annual evaporation ranges from about 1,500mm (Fiche station (2,300 masl) in the highlands of the sub-basin) to more than 6,800mm around Khartoum, the mouth of the subbasin [Sutcliffe, 1999]. Temperature and evaporation are observed to have good correlation with altitude. At high altitudes (>2300 masl) in the western highland plateau of Ethiopia mean annual temperature is reported to be in the range of 17°C to 19.5°C. Close to the Ethiopian-Sudan border where altitude is lowered to less than 1000 masl, temperature rises ranging from 24°C to 26.5°C. Around Khartoum, altitude is below 500 masl and temperature ranges from 28.5°C to 30.5°C.

3. Methodology

3.1 Metadata

In this study, precipitation simulations of the twentieth century (20c3m) from 16 of the global coupled atmosphere ocean general circulation models made available by the World Climate Research Program (WCRP) Coupled Model Inter-comparison Project phase 3 (CMIP3) *[Meehl et al., 2007]* were used in this study. 16 GCMs outputs were compared with observed CRU data for the period of 1901-2002.

GCMs normally run on a 3-dimensional grid with a horizontal resolution of 250-600 km, 10 to 20 vertical layers in the atmosphere and approximately 30 layers in the oceans [*Flato etal., 2000*]. Table 1 summarizes the 16 GCMs for which model output was used to construct forcing data for the hydrologic mode.

 Table 1. The Details of the Different GCM are used in this Study and their Spatial Resolutions (IPCC, 2007)

ID	Model Research Center	Model
1	Beijing Climate Center, China	BCCM1
2	Bjerknes Center for Climate Research, Norway	BCM2
3	Canadian Center for Climate Modelling and Analysis, Canada	CGMR
4	Centre National de Recherches Meteorologiques, France	CNCM3
5	Australia's Commonwealth Scientific and Industrial Research Organization, Australia	CSMK3
6	Metrological Institute of the University of Bonn, Germany (MIUB)	ECHOG
7	Geophysical Fluid Dynamics Laboratory, USA	GFCM20
8	Ocophysical Fluid Dynamics Laboratory, OSA	GFCM21
9	Goddard Institute for Space Studies, USA	GIER
10	UK Met Office, UK	HADCM3
11	OK Met Office, OK	HADGEM
12	Institute for Numerical Mathematics, Russia	INCM3
13	Institute Pierre Simon Laplace, France	IPCM3
14	National Institute for Environmental Studies, Japan	MIHR
15	Max-Planck-Institute for Meteorology, Germany	MPEH5
16	Meteorological Research Institute Japan	MRCGCM

3.2 Delta and Scaling Approach Correction

Statistical downscaling Method have been used to downscale and bias-correct the GCM data for both historical and future projection. The scaling approach is based on a simple ratio:

$$\Delta_{scale} = \frac{\overline{X}_{obs,1}}{\overline{X}_{sim 1}}$$
 1

With Δ _{scale} the scaling bias of variable X (here, the precipitation or relative humidity) over a 30-year baseline period (period 1) $\overline{X}_{obs,1}$ the average of the

baseline period (period 1), $X_{obs,1}$ the average of the observed variable X considered over period 1 and \overline{X} the average of the simulated environment X in the

 $\overline{X}_{\text{sim},1}$ the average of the simulated variable X in the same period 1. In order to correct for biases any simulated value of any period i of the climate model

considered with this scaling method, the following equation is followed:

2

$$X'_{sim,i} = X_{sim,i} * \Delta_{scale}$$

With X $_{sim,i}$ any modeled projection of variable X on any period i, and X' $_{sim,i}$ the bias-adjusted modeled projection of variable X on period i. With equation (2), the historical variability of the data is not excluded, thanks to the ratio considered in the scaling bias.

The value of X' $_{sim,i}$ obtained in the scaling approach is thus the fully bias-adjusted modeled projection of variable X, that reaches an appropriate bias corrected mean and variance with respect to the observed data.

3.3 Quantile Mapping Approach Correction

Wood et al. 2002 demonstrate that, statistical bias correction is carried out by first aggregating the gridded temperature and precipitation observations to the GCM grid scale (typically about 200 km resolution), and then using quantile mapping techniques to remove the systematic bias in the GCM simulations [Wood et al. 2002]. The quantile mapping (QM) method, proposed by Panofsy, H. A. and Brire, G.W. 1963, minimizes the differences between the observed/predicted data based on empirical probability distributions. Quantile mapping techniques work by creating a one-to-one mapping between two cumulative distribution functions (CDFs): one based on the GCM simulations and the second based on the aggregated observations. The mapping process is based on a simple nonparametric lookup procedure.

If the GCM simulation of temperature or precipitation for a particular month represents the estimated Xth quantile in the cumulative distribution function for the GCM simulations over a certain period, then the Xth quantile is looked up in the cumulative distribution function for the aggregated temperature or precipitation observations for the same period, and this new value becomes the "bias corrected" GCM value for that month. After applying this procedure, by construction, the bias corrected GCM simulations have the same CDF as the aggregated observations for the training period used to construct the two CDFs. It should be noted that no assumptions about the nature of the two probability distributions is required, and the process fully preserves the nature of the extremes in the observed CDF.

3.4 GCMs Performance

Five standard statistics, coefficient of determination (R^2), root mean square error (RMSE), standard deviation, bias on average and bias on standard deviation have been used to determine the performance of the GCMs.

Coefficient of determination (R2)

The square of the Pearson correlation coefficient (r^2) , known as the coefficient of determination, describes how much of the variance between the two variables is described by the linear fit.

$$R^{2} = \frac{\left(\sum_{i=1}^{n} (x_{i} - \overline{x}) \cdot (y_{i} - \overline{y})\right)^{2}}{\sum_{i=1}^{n} (x_{i} - \overline{x})^{2} \cdot \sum_{i=1}^{n} (y_{i} - \overline{y})^{2}} \qquad 3$$

Root mean square error (RMSE)

The Root Mean Square Error (RMSE) (also called the root mean square deviation, RMSD) is a frequently used measure of the difference between values predicted by a model and the values actually observed from the environment that is being modelled. These individual differences are also called residuals, and the RMSE serves to aggregate them into a single

measure of predictive power. The RMSE of a model prediction with respect to the estimated variable X_{model} is defined as the square root of the mean squared error:

$$RMSE = \sqrt{\frac{\sum_{i=1}^{n} (X_{obs,i} - X_{mo} del_{,i})^2}{n}} \qquad 4$$

where X_{obs} is observed values and X_{model} is modelled values at time/place i. However, the RMSE values can be used to distinguish model performance in a calibration period with that of a validation period as well as to compare the individual model performance to that of other predictive models.

4. Result and Discussion

Mean Monthly, Seasonal and Annual Precipitation

The observed mean monthly precipitation during baseline period was 132.38 mm/month over the Blue Nile. It is evident that many of the models either overestimated or underestimated the rainfall while some were even unable to reproduce the seasonal cycle. Most models output are more than observed value over the Blue Nile. Figure 2 shows the 30 years monthly precipitation normal period (1971 - 2000) of the observed and 16 GCM over the Blue Nile. It can be seen that the trends of the modes output vary in a big range. Most of the simulations in May, June, July, August and September are less than the observation. There is a range of model performance ranging from wet biases in every month (e.g. Bjerknes Centre for Climate Research (BCCR) and CNCM3 (Meteo-France) through to dry biases in most months BCCM1 (Beijing Climate Center, China). Four of these models BCM2 (Bjerknes Centre for Climate Research, Norway), CGMR (Canadian Centre for Climate Modeling & Analysis), CNCM3 (Meteo-France) and HADGEM (Met Office Hadley Centre, UK) gave the maximum precipitation over the Blue Nile in August, which is in the line with the observation. It can be noticed that HADGEM have the most/ consistent variability over the Blue Nile with observation as seen in Figure 2.

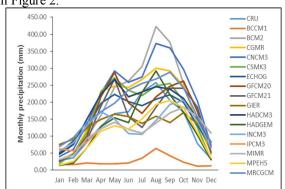


Figure 2. Monthly Rainfall comparison between CRU and 16 GCMs

Comparisons of mean monthly precipitation (MMP), mean seasonal precipitation (MSP) and mean annual precipitation (MAP) between GCM estimates and observed data during the period 1971-2000 are presented in Table 2. For the mean monthly precipitation (MAP) over the Blue Nile, the correlation coefficient CC varies from a maximum of 0.98 ($R^2 = 0.96$) with a RMSE value of 18.23 mm/month for model HADGEM (Met Office Hadley Centre, UK) to 0.58 for INCM3 (Institute of Numerical Mathematics, Russian Academy of Sciences) with R² value of 0.34 and RMSE of 40.93 mm/month. While, for the mean seasonal precipitation (MSP), the correlation coefficient CC varies between 0.995 - 0.710. Whereas BCM2 (Bjerknes Centre for Climate Research, Norway) has the best performance model with coefficient of determination ($R^2 = 0.99$) and RMSE value of 0.35 mm/season, followed by HADGEM (UK Met Office) (R²=0.99 and RMSE=0.35) and IPCM3 (Institute Pierre Simon Laplace, France) has the poor performance GCM $(R^2=0.5 \text{ and } RMSE=1.01)$. CGMR (Canadian Centre for Climate Modeling & Analysis) (CC=0.53, $R^2=0.28$, RMES=96.18 mm/year) and GFCM21 (Meteorological Research Institute, Japan) (CC=-0.38, $R^2=0.15$, RMES=69.48 mm/year) are found to be the best and poorly performing GCM in terms of mean annual precipitation, respectively Table 2. The rank of the GCM models for the mean monthly, seasonal and annual precipitation are summarized in Table 2. These higher-ranking models are the logical candidates for driving off-line simulations of simulated projected time horizon. The best five GCM models are highlighted in green, blue, gold assent 4, yellow and orange assent 2

Bias Correction 1 "Scaling Approach

For each 30-year mean monthly precipitation (MMP), mean seasonal precipitation (MSP) and mean

annual precipitation (MAP) over the 1971-2000 period, the Δ biases have been calculated based on the mean and standard deviation and displayed on Table 3. It is clear that HADGEM family of the Meto Office, UK performs better than other model over the Blue Nile for simulating precipitation.

It is noticed that HADGEM model performs the best in 4 months (April, July, October and November) and is consider the second best model in May and December. Also is consider the third best model in August and September (Table 3).

For winter "December-February" (DJF) over the Blue Nile, it is noticed from Table 4, that CSMK has the best performance (1.04 mm/season), while the GEIR has the weakness performance (2.59 mm/season) over the nominal period 1971-200. But for spring "March-May" (MAM), BCM2 (Bjerknes Centre for Climate Research, Norway) and CGMR (Canadian Centre for Climate Modeling & Analysis) are considered the best and poorly performing performance, respectively. While HADGEM and GIER have the best performance among the 16 GCM for simulating summer "June-August" (JJA), and autumn "September-November" (SON), respectively. It is noticed that MPEH5 (Max Planck Institute for Meteorology, Germany) and HADGEM performs better than other models during the Dry Season, but CNCM3 has the weakness performance. While HADGEM and BCM2 is considered the best and poorly performing performance during the Wet Season. Therefore, HADGEM (Met Office Hadley Centre), UK have been selected as the best model to simulate Blue Nile for its overall performance for seasonal, monthly and annual.

Bias Correction 2 "Quantile Mapping Approach

Figure 3 illustrates the CDF comparison between the observed/ or historical and the simulated GCMs models over the Blue Nile.

h Concurrent Observed Data over the Blue Nile														
	Mean Monthly Precipitation					Mean Seasonal Precipitation				Mean Annual Precipitation				
Model	MMP				MSP				MAP					
	CC	\mathbf{R}^2	RMSE	RANK	CC	\mathbf{R}^2	RMSE	RANK	CC	\mathbf{R}^2	RMSE	RANK		
BCCM1	0.809	0.65	9.3	10	0.934	0.87	0.18	9	-0.14	0.02	33.68	8		
BCM2	0.964	0.92	36.69	3	0.995	0.99	0.45	1	-0.10	0.01	148.36	9		
CGMR	0.964	0.93	27.89	2	0.983	0.97	0.61	5	0.53	0.28	96.18	1		
CNCM3	0.945	0.89	39.05	5	0.984	0.97	0.66	3	0.09	0.01	212.75	10		
CSMK3	0.901	0.81	42.44	8	0.932	0.87	1.07	10	0.10	0.01	105.02	11		
ECHOG	0.896	0.80	29.25	9	0.937	0.88	0.73	7	0.04	0.00	113.75	14		
GFCM20	0.785	0.62	67.85	12	0.861	0.74	1.29	11	-0.01	0.00	145.98	15		
GFCM21	0.693	0.48	62.28	13	0.818	0.67	1.25	14	-0.02	0.00	136.83	16		
GIER	0.804	0.64	20.10	11	0.844	0.71	0.62	12	-0.10	0.01	85.84	12		
HADCM3	0.903	0.82	33.74	7	0.937	0.88	0.85	8	0.26	0.07	98.17	5		
HADGEM	0.980	0.96	18.23	1	0.993	0.99	0.35	2	0.32	0.10	113.12	3		
INCM3	0.589	0.34	40.94	16	0.842	0.71	0.61	13	-0.27	0.07	133.27	6		
IPCM3	0.597	0.35	33.88	15	0.710	0.50	1.01	16	0.25	0.06	106.36	7		

 Table 2. Performance Statistics Comparing CMIP3 GCM Mean Monthly, Seasonal and Annual Precipitation with Concurrent Observed Data over the Blue Nile

Model	Mean MMP	Month	y Precipit	tation	Mean MSP	Season	al Precipi	tation	Mean Annual Precipitation MAP			
	CC	R ²	RMSE	RANK	CC	R ²	RMSE	RANK	CC	R ²	RMSE	RANK
MIMR	0.618	0.38	38.07	14	0.711	0.51	1.02	15	-0.08	0.01	178.38	13
MPEH5	0.920	0.84	26.84	6	0.973	0.95	0.49	6	-0.30	0.09	81.45	4
MRCGCM	0.961	0.92	21.82	4	0.992	0.98	0.35	3	-0.38	0.15	69.48	2

On this table, the results highlighted in different color according to their rank

Color	Key
	Rank 1
	Rank 2
	Rank 3
	Rank 4
	Rank 5

Table 3. Bias for Rainfall between CMIP3 GCM Model Simulations and CRU Observation (1971-2000) Over the Blue Nile.

Madal	Mean Monthly Precipitation MMP				Mean S MSP	Seasonal Pre	cipitation		Mean Annual Precipitation MAP				
Model	μ*	σ**	Bias on µ	Bias on σ	μ*	σ**	Bias on μ	Bias on σ	μ*	σ**	Bias on μ	Bias on σ	
BCCM1	25.0	15.1	0.2	0.2	0.8	0.5	0.2	0.2	301.2	33.4	0.2	0.3	
BCM2	202.0	131.5	1.5	1.6	6.7	4.0	1.5	1.6	2422	146.7	1.5	1.4	
CGMR	184.7	100.9	1.4	1.3	6.1	3.0	1.4	1.2	2210	111.5	1.4	1.1	
CNCM3	216.2	114.8	1.6	1.4	7.1	3.4	1.6	1.4	2605	210.1	1.6	2.0	
CSMK3	166.5	93.7	1.3	1.2	5.5	2.7	1.3	1.1	1994	103.7	1.3	1.0	
ECHOG	158.6	63.0	1.2	0.8	5.1	1.9	1.2	0.8	1905	112.0	1.2	1.1	
GFCM20	165.8	89.2	1.3	1.1	5.4	2.3	1.2	0.9	1987	143.5	1.3	1.4	
GFCM21	150.3	82.4	1.1	1.0	4.9	1.9	1.1	0.8	1806	134.6	1.1	1.3	
GIER	132.4	32.3	1.0	0.4	4.2	1.0	1.0	0.4	1587	84.8	1.0	0.8	
HADCM3	178.0	75.1	1.3	0.9	5.8	2.2	1.3	0.9	213	99.8	1.3	0.9	
HADGEM	130.7	88.8	1.0	1.1	4.4	2.7	1.0	1.1	1562	117.3	1.0	1.1	
INCM3	129.8	48.3	1.0	0.6	4.1	1.0	0.9	0.4	1557	136.2	1.0	1.3	
IPCM3	120.9	40.3	0.9	0.5	3.8	1.3	0.9	0.5	1448	108.0	0.9	1.0	
MIMR	118.2	46.2	0.9	0.6	3.8	1.3	0.9	0.5	2245	176.0	1.4	1.7	
MPEH5	112.7	65.5	0.9	0.8	3.7	1.9	0.9	0.8	1354	83.9	0.9	0.8	
MRCGCM	183.6	76.0	1.4	1.0	6.0	2.5	1.4	1.0	2204	74.0	1.4	0.7	
CRU	132.4	79.9	1.0	1.0	4.4	2.5	1.0	1.0	1584	105.4	1.0	1.0	

On this table, the results highlighted in green show the smallest biases.

* μ = mean, ** σ = Std. deviation

Similar to the previous section, it is obviously seen from Figure 3, that HADGEM (Meto Office, UK, Figure 3 (k) has the smallest bias among the 16 models, which mean that HADGEM has the best performance over the Blue Nile for simulating precipitation.

Table 4. Bias (△ scale) for Seasonal and Annual Rainfall between CMIP3 GCM Model Simulations and CRU
Observation (1971-2000) Over the Blue Nile

GCM	DJF	MAM	JJA	SON	Dry Season	Wet Season	Annual
BCCM1	0.20	0.13	0.37	0.05	0.17	0.26	0.20
BCM2	1.21	1.05	3.58	4.05	1.35	3.69	2.23
CGMR	1.49	2.50	1.70	1.35	1.78	1.78	1.78
CNCM3	1.80	1.73	1.38	1.89	1.85	1.51	1.63
CSMK3	1.04	1.62	1.07	1.28	1.38	1.19	1.26
ECHOG	2.12	1.44	0.91	1.22	1.53	1.02	1.20
GFCM20	1.29	1.60	0.88	1.50	1.57	1.08	1.25
GFCM21	1.28	1.44	0.71	1.46	1.48	0.95	1.13
GIER	2.59	1.16	0.69	0.98	1.48	0.74	1.00
HADCM3	2.10	1.70	1.05	1.32	1.68	1.16	1.34

HADGEM	0.68	0.92	1.00	1.09	0.95	1.01	0.99
INCM3	2.08	1.20	0.54	1.19	1.53	0.68	0.98
IPCM3	2.35	0.91	0.56	1.12	1.39	0.66	0.91
MIMR	1.90	0.94	0.56	1.12	1.33	0.66	0.89
MPEH5	0.79	0.82	0.71	1.10	0.99	0.78	0.85
MRCGCM	2.55	1.35	1.15	1.51	1.71	1.21	1.39

On this table, the results highlighted in green show the smallest biases, in yellow second smallest bias and in Orange third smallest bias for GCM

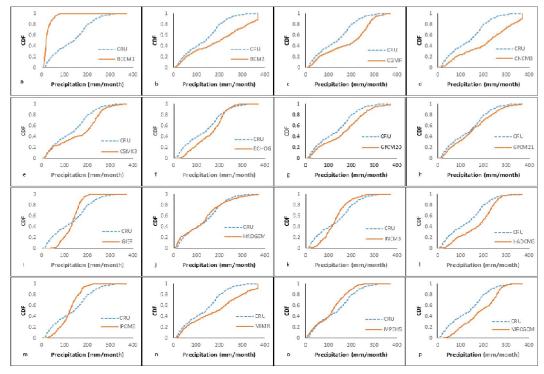


Figure 3. CDF Comparison between CRU and 16 GCMs over the Blue Nile (1971-2000)

Skill Assessment of GCM Simulation in the Near, Intermediate and Far Future Period

The difference between GCM simulated and observed rainfall over the Eastern Nile was analyzed using the time horizon 2020s (2010–2039), the 2050s (2040–2069) and the 2080s (2070–2099) representing near, intermediate and far future, respectively, while comparing them to the end of the 20th century climate normals (1971-2000). Table 5 illustrates mean monthly rainfall and standard deviation rainfall of simulated the 16 GCM models during projected time horizons as well as rainfall tend over the Blue Nile.

Mean Monthly and Seasonal Precipitation

By omitting BCCM1 model, the minimum and maximum monthly rainfall change for the Blue Nile are -1,89% and +63.57%, -5.96% and +69.37%, and -8.9% and +76.44% for future periods 2010–2039, 2040–2069 and 2070–2099, respectively (Table 5). These results are in contrast to the results of *Beyene*, *et al.*, 2010. He investigated that the climate models

predict precipitation changes under the same global emission scenarios A2 by 2070 between -34% and +24% compared to a longer nominal period 1950-1999. However, according to ElShamv et al., 2009, over the longer term (2081–2098), the Blue Nile Basin may become drier. Using the outputs from 17 GCM for the A1B scenario their predictions varied between a -15% and +14% change in precipitation, with the ensemble mean suggesting little change. This large uncertainty is mirrored in other studies and reflects the difficulty of downscaling from global models to regional levels, but also indicates lack of understanding of phenomena like ENSO, which are important for the Eastern African climate. 7 GCM Model expected less rainfall in 2040-2069 than 2010-2039. Table 5 illustrates the five best performance climate models over the Blue Nile. The minimum and maximum monthly rainfall change are -1,87% and +3.75%, -1.45% and +2.48%, and -1.99% and +5.04% for future periods 2010-2039, 2040-2069 and 20702099, respectively. The negative sign indicates that the basin will be drier due to generally increased rainfall, while the positive sign indicates that the basin will be wetter due to generally increased rainfall. 11 GCM model of the 16 indicate that Blue Nile Basin is wetter in the first period of the 21st century 2020s (2010-2039), while 12 GCM models and 9 models shows that Blue Nile Basin is wetter the in the second and third period compared to the nominal period (1971-2000). The Blue Nile sub basin mean monthly rainfall based on the best performance climate model HADGEM downscaling were -1.87%, +1.62% and +4.71% of observed historical rainfall (1971-2000) for future periods of 2020s (2010-2039), 2050s (2040-2069) and 2080s (2070-2099). During the first half of the 21st century the pattern of the rain is drier, while wetter condition in the second and last half of the 21st century. These results are in contrast to the results of CGMR downscaling, which showed a consistent increase and decrease of +1.48, +0.66 and -1.99% for 2010-2039 (near future), 2041-2070 (intermediate future) and 2071-2100 (far future), respectively. the mean monthly rainfall of the simulated BCM2 and CGMR are projected to decrease by 2080s (20702099) over the Blue Nile, while the mean monthly rainfall of the HADGEM, MRCGCM and CNCM3 are projected to increase by the end of the 21st century. The expected decrease of simulated BCM2 and CGMR are 1.45% and 1.99%, respectively. However, the expected increase of simulated HADGEM, MRCGCM and CNCM3 are 4.71%, 4.53% and 5.04%, respectively. The mean monthly rainfall of the best climate model, HADGEM (Met Office Hadley Centre, UK) over the Blue Nile varies between 128.31 to 136.91 mm/month (Figure 4). Compared to the 20th century climate normals (1971-2000) an increase of 1.62% and 4.7% was observed by 2050s (2040-2069) and 2080s (2070-2099), respectively (Figure 5). Averaged across GCM models for SRES A2 global emissions scenarios and for periods 2010-2039 to 2070-2099, multimodal averages suggest that the Blue Nile Sub-basin regions will experience increases in JJA rainfall in the late 21st Century (Figure 6). These results relevant to Bevene, et al., 2010 investigation, he suggested that the effects of climate change would cause the basin to become wetter in winter (DJF) in both the Blue and mixed results in the summer (JJA).

 Table 5. Mean, Standard Deviation and Rainfall Change for the Region of Interest over the Blue Nile

Model	1971-200	0	2010-203	9		2040-206	59		2070-2099		
Widdei	Mean	Std	Mean	Std	PI	Mean	Std	PI	Mean	Std	PI
BCCM1	25.05	15.11	11.21	4.79	-55.25				0.00	0.00	
BCM2	201.99	131.53	199.50	125.82	-1.23	199.06	130.44	-1.45	199.06	130.44	-1.45
CGMR	184.66	100.92	187.40	99.27	1.48	185.89	96.68	0.66	180.99	95.06	-1.99
CNCM3	216.16	114.78	217.26	115.21	0.51	217.53	117.35	0.63	227.06	115.37	5.04
CSMK3	166.51	93.70	217.26	115.21	30.48	160.47	94.22	-3.63	162.95	93.97	-2.14
ECHOG	158.57	63.05	162.07	63.91	2.21	168.89	69.90	6.51	174.33	76.75	9.94
GFCM20	165.83	89.19	165.60	92.03	-0.13	155.94	80.99	-5.96	151.07	74.11	-8.90
GFCM21	150.25	82.44	147.28	82.92	-1.98	144.59	79.94	-3.77	147.51	81.71	-1.82
GIER	132.39	32.28	136.07	32.34	2.78	139.68	30.83	5.51	151.56	33.53	14.48
HADCM3	178.03	75.06	181.81	72.05	2.12	186.37	72.18	4.68	198.44	73.92	11.47
HADGEM	130.75	88.82	128.31	88.21	-1.87	132.87	93.16	1.62	136.91	103.12	4.71
INCM3	129.81	48.31	140.56	54.91	8.28	134.24	58.25	3.41	148.02	67.28	14.02
IPCM3	120.93	40.29	121.38	41.62	0.37	123.20	43.76	1.88	121.77	40.01	0.70
MIMR	118.22	46.17	193.37	116.72	63.57	200.22	123.03	69.37	208.59	124.01	76.44

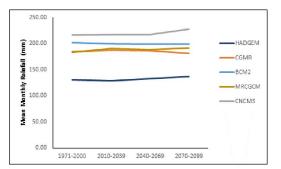
On this table, the results highlighted in different color according to their rank

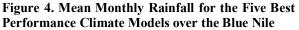
Color	Key
	Rank 1
	Rank 2
	Rank 3
	Rank 4
	Rank 5

5. Conclusion and Recommendation

This paper assesses the capability of GCMs with A2 emission scenario to simulate the current climate and compares the future climate change predictions over the Blue Nile Basin. Sixteen GCM runs were evaluated for capability to simulate observed mean monthly mean seasonal and mean annual precipitation for the 1971-2000 period. However, the better performing GCMs were identified by estimating the difference between the GCMs and observed mean monthly rainfalls. The indicators used to evaluate the GCMs performance were correlation coefficient, R² and RMSEs, mean and the standard deviation of mean monthly mean seasonal and mean annual precipitation. The difference between GCMs were significant. The correlation coefficients, R² were high for most five best performance models (HADGEM, CGMR, BCM2, MRCGM and CNCM3) and the PRMSE was generally low, while the rest of the models give a vise versa results. The future simulations were conducted for 2020s (2011–2039), 2050s (2041–2070) and 2080s (2071–2100) horizons representing near, intermediate and far future, respectively and were compared with 1970–2000 CRU nominal period.

During the first half of the 21^{st} century, the pattern of the rain of HADGEM is drier, while wetter condition in the second and last half of the 21^{st} century. The mean monthly rainfall change of HADGEM (best performance model) downscaling were -1.87%, +1.62% and +4.71% of observed historical rainfall (1971-2000) for future periods of 2020s (2010–2039), 2050s (2040–2069) and 2080s (2070–2099). The correlation coefficient, R² and RMSE for the mean monthly precipitation (MAP) were 0.98%, 0.96% and 18.23 mm/month. The results of this paper can be used as an input to hydrological models for predicting the flow at the Blue Nile by the end of the 21^{th} century as a tools for decision support system.





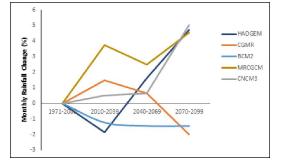


Figure 5. Monthly Rainfall Change for the Five Best Performance Climate Models over the Blue Nile

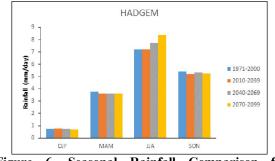


Figure 6. Seasonal Rainfall Comparison for HADGEM (Rank 1) Over the Blue Nile

Acknowledgements

The authors would like to thank the Dr.Ir. (Assistant Professor) Herbert ter Maat from Alterra Wageningen UR, The Netherlands for guidance for downscaling global climate model and bias correction and providing the data of the model predictions used in this present study.

Reference

- Beyene, T., Lettenmaier, D. P., and Kabat, P. (2010). Hydrologic Impacts of Climate Change on the Nile River Basin: Implications of the 2007 IPCC Scenarios, Climatic Change, 100, 433–461.
- Chiew, F. H. S., Kirono, D. G. C., Kent, D. M., Frost, A. J., Charles, S. P., Timbal, B., Nguyen, K. C. & Fu, G. (2010). Comparison of Runoff Modelled using Rainfall from Different Downscaling Methods for Historical and Future Climates. J. Hydrol. 387 (1–2), 10–23.
- Chiew, F. H. S., Teng, J., Vaze, J. & Kirono, D. G. C. (2009). Influence of Global Climate Model Selection on Runoff Impact Assessment. J. Hydrol. 379 (1–2), 172–180.
- Christensen, N. S., Lettenmaier, D.P. (2007). A Multimodal Ensemble Approach to Assessment of Climate Change Impacts on the Hydrology and Water Resources of the Colorado River Basin, Hydrology and Earth System Sciences, 11(4):14171434.
- Conway, D. (2005). From Headwater Tributaries to International River: Observing and Adapting to Climate Variability and Change in the Nile Basin. Global Environmental Change, 15 (2): 99-114.
- Conway, D. (1997). A Water Balance Model of the Blue Nile in Ethiopia. Hydrol. Sci. J., 42, 265–286.
- Elshamy, M. E., Seierstad, I. A. en Sorteberg, and A. (2009). Impacts of Climate Change on Blue Nile Flows using Bias Corrected GCM Scenarios. University of Bergen, Norway: Hydrology and Earth System Sciences, 2009.
- Flato, G.M., G.J. Boer, W.G. Lee, N.A. McFarlane, D. Ramsden, M.C. Reader, and A.J. Weaver. (2000). The Canadian Centre for Climate Modeling and Analysis Global Coupled Model and its Climate. Climate Dynamics, 16:451-467.

- Harpham, C. & Wilby, R. L. (2005). Multi-site Downscaling of Heavy Daily Precipitation Occurrence and Amounts. J. Hydrol. 312 (1–4), 235–255.
- Hulme, M., R. Doherty, T. Ngara and M. New, (2005). Global Warming and African Climate Change. Climate Change and Africa, P.S Low, Ed., Cambridge University Press, Cambridge, 29-40.
- IPCC (2014). Climate Change 2014: Impacts, Adaptation, and Vulnerability. In: Working Group II to the Fifth Assessment Report of the Intergovernmental Panel on Climate. Edit by Vicente R. Barros, Christopher B. Field, David Jon Dokken, Michael D. Mastrandrea, Katharine J. Mach. Cambridge University Press, Cambridge, UK.
- IPCC (2007). Climate Change 2007: Impacts, Adaptation, and Vulnerability. In: Working Group II to the Fourth Assessment Report of the Intergovernmental Panel on Climate Change. Edit by Parry ML, Canziani OF, Palutikof JP, van der Linden PJ, Hanson CE, eds. Cambridge: Cambridge University Press, Cambridge, UK.
- IPCC (2001). Climate Change 2001: Impacts, Adaptation, and Vulnerability. In: Working Group II to the Third Assessment Report of the Intergovernmental Panel on Climate Change. Edit by J. J. McCarthy, O. F. Canziani, N. A. Leary, D. J. Dokken & K. S. White). Cambridge University Press, Cambridge, UK.
- Khan, M. S., Coulibaly, P. & Dibike, Y. (2006). Uncertainty Analysis of Statistical Downscaling Methods. J. Hydro. 319(1–4), 357–382
- Kundzewicz Z. W., and Mat L. J. (2007). Freshwater Resources and Their Management, in Climate Change 2007: Impacts, Adaptation and Vulnerability-Contribution of Working Group II to the Fourth Assessment Report of the Intergovernmental Panel on Climate Changel, pp. 174–210, Cambridge Univ. Press, Cambridge, U. K. (2007).
- Mearns, L. O., M. Hulme, T. R. Carter, R. Leemans, M. Lal, and P. Whetton. (2001): Climate Scenario Development (Chapter 13). In Climate Change 2001: The Scientific Basis, Contribution of Working Group I to the Third Assessment Report of the IPCC [Houghton, J. T., Y. Ding, D. J. Griggs, M. Noguer, P. J. van der Linden, X. Dai, K. Maskell, and C. A. Johnson (eds.)]. Cambridge U. Press: Cambridge, pp. 583-638.
- Meehl, G.A., T.F. Stocker, W.D. Collins, P. Friedlingstein, A.T. Gaye, J.M. Gregory, A. Kitoh, R. Knutti, J.M. Murphy, A. Noda, S.C.B. Raper, I.G. Watterson, A.J. Weaver and Z.-C. Zhao. (2007). Global Climate Projections. In: Climate Change 2007: The Physical Science Basis. Contribution of Working Group I to the Fourth Assessment Report of the Intergovernmental Panel on Climate Change [Solomon, S., D. Qin, M. Manning, Z. Chen, M.

12/12/2015

Marquis, K.B. Averyt, M. Tignor and H.L. Miller (eds.)]. Cambridge University Press, Cambridge, United Kingdom and New York, NY, USA.

- Mishra A, Hata T, Abdelhadi AW, Tada A, and Tanakamaru H. (2003). Recession Flow Analysis of the Blue Nile River," Hydrological Processes, Special issue: Japan Society of Hydrology and Water Resources, vol. 17, 2003.
- 19. Peggy, A.J. and Curtis, D. (1994). Water Balance of the Blue Nile Basin in Ethiopia," Journal of Irrigation and Drainage Engineering, vol. 120, no. 3, pp. 573-590, 1994.
- Perkins, S. E., Pitman, A. J., Holbrook, N. J. & Mcaneney, J. (2007). Evaluation of the AR4 climate models' simulated daily maximum temperature, minimum temperature, and precipitation over Australia using probability density functions. J. Climate 20, 4356–4376.
- Gebrehiwot S .G., Ilstedt U., Gardenas A. I. and Bishop K. (2011). Hydrological Characterization of Watersheds in the Blue Nile Basin, Ethiopia. Hydrol. Earth Syst. Sci., 15, 11–20.
- 22. Schiermeier, Q. (2010). The Real Holes in Climate Science. Nature, 463, 284-287.
- 23. Shahin M. (1985). Hydrology of the Nile Basin. Elsevier Science Publishers BV/Science and Techno logy Division, Amsterdam, the Netherland, 1985.
- 24. Sutcliffe J. V. and Parks Y. P.(1999). The Hydrology of the Nile. IAHS Specific Publications, no. 5, 1999.
- Timbal, B., Fernandez, E. & Li, Z. (2009) Generalization of a statistical downscaling model to provide local climate change projections for Australia. Environ. Model. Softw. 24(3), 341–358.
- UNS (2007). World Population Prospects: The 2006 Revision and World Urbanization Prospects: The 2007 Revision [Online]. Available: http://esa.un.org/unup/ [Accessed Monday, October 19, 2009]. United Nations Secretariat.
- Whitehead, P. G., Wilby, R. L., Butterfield, D. & Wade, A. J. (2006). Impacts of Climate Change on instream Nitrogen in a Lowland Chalk Stream: An Appraisal of Adaptation Strategies. Sci. Total Environ. 365 (1–3), 260–273.
- Whittington, D., Guariso, G. (1983). Water Management Models in Practice: A Case Study of the Aswan High Dam. Elsevier Scientific Publishing Company, Amsterdam, 1983.
- Wilby, R. L., Dawson, C. W. & Barrow, E. M. (2002) SDSM – A Decision Support Tool for the Assessment of Regional Climate Change Impacts. Environ. Model. Softw. 17(2), 145–157.
- Wood, A. W., Maurer, E. P., Kumar, A., and Lettenmaier, D. P. (2002). Long-range Experimental Hydrologic Forecasting for The Eastern United States, J. Geophys Res., 107, 4429, doi:4410.1029/2001JD000659.